The Surface Chemical Properties of Novel High Surface Area Solids Synthesized from Coal Fly Ash

P. Julius Pretorius[a†] and Christopher D. Woolard[b*]

[a] *Division of Water, Environment and Forestry Technology, CSIR, P.O. Box 320, Stellenbosch, 7599 South Africa.*

[b] *Department of Chemistry, University of Port Elizabeth, Port Elizabeth, 6031 South Africa.*

Received 12 March 2002; revised 6 January 2003; accepted 20 January 2003.

ABSTRACT

The zeolite, Na-P1, was synthesized from fly ash samples originating from coal-fired power stations in South Africa by hydrothermal treatment of the raw ash with concentrated aqueous NaOH solutions. The zeolite was then further modified by acid leaching at elevated temperatures. This resulted in the formation of a novel high surface-area solid. Spectroscopic and potentiometric investigations into the surface properties of both solids indicate that acid-base properties are most likely due to the presence of ≡AlOH- and ≡SiOH-type surface groups. Surface protonation constants for the various solids (unmodified ash, base-modified ash, acid-etched zeolitic product) are reported. Metal sorption studies were performed for cadmium and copper. It is suggested that the zeolitic product sorbs copper and cadmium by an ion exchange mechanism instead of a surface complexation mechanism, whereas the high surface-area solid, formed after acid etching, sorbs these metals *via* a surface complexation mechanism. Metal adsorption constants for the formation of ≡XOMOH species on the surface of the last mentioned solid for use in speciation models are reported.

KEYWORDS

Fly ash, surface complexation model, metal complexation, waste beneficiation, surface characterization.

1. Introduction

It has been projected that by the year 2000 the production of coal fly ash in the United States alone will have reached 150 million tonnes per annum.[1] In South Africa, where coal with a high ash content is used in power generation, 25 million tonnes of fly ash were produced in 2000. Only 5% of this ash was sold for re-use.[2] Most fly ash is disposed in solid waste landfills or surface impoundments.[3] Attempts to recycle the material have focussed on using it as a soil amendment material, a cement extension in the building and construction industries, as a toxic element immobilizer in the waste management industry and as a filler in the polymer industry.[1,4]

It has been observed that heat treatment of fly ash in an alkali environment results in the formation of zeolites.[3,5–10] Pure zeolites themselves have shown promise as materials for nuclear waste processing.[11] Because these zeolitized fly ashes also exhibit high cation exchange capacity, it has been proposed that these materials may be used as permeable liners for hazardous waste disposal sites or agents for the removal of trace metals from industrial wastewaters.[8]

The successful use of fly ash, or modifications thereof, for the above purposes depends on the surface chemical properties of the solid. The measurement of adsorption constants for the protonation of various solid sorbents as well as those for metal adsorption allows for the prediction of heavy metal speciation by inclusion of such constants into speciation programs such as MINTEQA2[12] and hence predictions about bioavailability and biotoxicity can be made. Such constants are readily available for compounds which are adsorbed by a surface complexation mechanism with surface hydroxyl groups, e.g. metals onto hydrous ferric oxides.[13] Such constants, however, are presently not available for the adsorption of various species onto fly ash and its derivatized products. Before speciation calculations can be conducted on systems containing either fly ash or modified products, adsorption constants need to be determined. At present, investigations of the surface of fly ash and derived products do not extend beyond morphological observations and the measurement of cation exchange capacities.

In this paper we report on the synthesis of modified fly ash samples, including the use of acid etching to provide a novel high surface-area material. We report on the nature of the ash and product surface through the use of a variety of spectroscopic techniques. Potentiometric results are then presented together with protonation constants for the various solids. We discuss the mechanism of metal sorption and then present surface complexation constants for Cu and Cd onto the high surface-area acid-etched solid.

2. Experimental

2.1. Ash Modification

Two pulverized, unmodified fly ash (UFA) samples (particle size ≤5 μm) were obtained from Ash Resources, South Africa. Samples MFA1 and MFA2 were modified according to a modification of the procedure of Amrhein *et al.*[3] This entailed refluxing an amount of raw ash in a concentrated alkali solution. 40 g of fly ash was mixed with 400 cm^3 NaOH (1 mol dm^{-3} and 2 mol dm^{-3} for MFA1 and MFA2 respectively) and the mixture was refluxed at ambient pressure for 21 h (MFA1) and 72 h (MFA2) with continuous stirring. The resulting slurry was filtered using a 0.22 μm membrane filter (Millipore) and the solid was washed repeatedly with deionized water before being dried under vacuum at 60°C for 24 h. A high surface-area sample, MFA3, was prepared by refluxing a sub-sample of MFA1 with 3 mol dm^{-3} HCl for 6.5 h. The slurry was washed, filtered and dried as before.

* To whom correspondence should be addressed: E-mail chacdw@upe.ac.za
† Now: Sasol Technology, P.O. Box 1, Sasolburg, 1947 South Africa.

2.2. Physical Characterization

Elemental compositions of the samples were determined by X-ray fluorescence spectrometry on a Philips PW1480 X'Unique 11 automatic sequential spectrometer. Sample mineralogy was investigated by X-ray diffraction (XRD) spectrometry using a Rigaku diffractometer and CuK_α radiation ($\lambda = 1.542$ Å). Surface properties were investigated using scanning X-ray photoelectron spectroscopy (SXPS). Spectra were collected on a Quantum 2000 Scanning ESCA Microprobe. Scanning electron microscopy (SEM) was performed on a Philips XL 30 scanning electron microscope to which an EDAX DX4 energy dispersive X-ray analyser system (EDS) was coupled, which also allowed elemental compositions to be estimated.

2.3. Potentiometric Titrations

Approximately 0.05 g of the solid was accurately weighed out and transferred to a thermostatted pyrex titration vessel containing 20.00 cm^3 of 0.3 mol dm^{-3} $NaNO_3$ (Merck GR) and 2.00 cm^3 of 0.1 mol dm^{-3} NaOH in a 0.3 mol dm^{-3} $NaNO_3$ background electrolyte solution. For metal adsorption studies, an additional 2.00 cm^3 of stock metal solution was added to the titration vessel. The suspension was stirred continuously using a magnetic stirrer and Teflon-coated stirrer bar. Titrations were started as soon as the suspension pH stabilized at 25°C. All titrations were performed under N_2 atmosphere. The EMF in the vessel was measured by a computer-controlled pHM64 Research pH meter (Radiometer) connected to a glass electrode and a calomel reference electrode (both Radiometer). The electrode system was calibrated in terms of hydrogen ion activity according to the IUPAC pH scale, using buffers at pH 4.01, 7.00 and 9.18 (Radiometer). Titrant (0.1 mol dm^{-3} HNO_3) was added with a computer controlled ABU80 automatic burette (Radiometer). An increment of titrant was added once the EMF drift was less than 0.1 mV per 20 s, or after 180 s, depending on which condition was satisfied first.

2.4. Batch Metal Sorption Experiments

Cadmium sorption by MFA2 was investigated over a range of metal concentrations at pH 5.7, 7.4 and 9.5 at a background electrolyte concentration of 0.3 mol dm^{-3} $NaNO_3$ (Merck GR) at 25°C. Metal concentrations ranging from 1.0×10^{-3} mol dm^{-3} to 1.0×10^{-6} mol dm^{-3} were brought into contact with a 2 g dm^{-3} suspension of MFA2. The suspension was covered and agitated with a mechanical shaker for 24 h, after which the suspension was filtered over a 0.45 μm membrane filter (Millipore). The filtrate was analysed using graphite furnace atomic absorption spectrometry (GFAAS). The quantity of metal sorbed was calculated by difference.

2.5. Adsorption Constant Determinations

Protonation constants were determined from the potentiometric titration data using the non-linear iterative optimization program FITEQL.[14] Input data consisted of (a) total hydrogen ion concentration, T_H, (b) the logarithm of free hydrogen ion concentration, log[H^+], (c) dilution factors and (d) the mass of solid (g dm^{-3}). Surface protonation constants and surface site concentrations were calculated from these data.

The surface protonation constants and surface site concentrations were then used with similar data from metal titration experiments as well as the total metal concentration, T_M, to optimize metal adsorption constants. Equilibrium constants for solution phase reactions were corrected to an ionic strength of 0.3 mol dm^{-3} using the extended Debye-Hückel equation in the speciation program, MINTEQA2.[12]

Model selection was based on (a) the value of the goodness of fit parameter WSOS/DF (i.e. the weighted square of sums of the differences divided by the number of degrees of freedom) calculated in FITEQL, and (b) the standard deviations of the calculated log K values, which were required to satisfy the criterion $\sigma_{logK} \leq 0.15$.

Table 1 Elemental composition of raw and modified fly ash.

Element	Concentration/mass %				
	Raw fly ash		Treated fly ash		
	UFA1	UFA2	MFA1	MFA2	MFA3
Na	0.24	0.24	6.39	7.14	6.37
Mg	0.42	0.99	0.55	0.73	0.00
Al	14.93	18.75	15.89	16.91	13.68
Si	19.76	24.14	17.95	16.63	26.82
Ca	2.40	2.90	2.08	2.67	0.03
Cr	5.01	0.03	5.02	0.03	5.89
Fe	1.68	2.01	1.93	1.85	0.27
Ni	2.75	0.01	1.41	0.01	0.11
Si/Al	1.32	1.29	1.14	0.98	1.96

3. Results and Discussion

3.1. Ash Modification

Representative elemental analyses of the raw and modified ash samples are shown in Table 1. Treatment of the unmodified fly ash (UFA) results in changes in the elemental composition of the sample, indicating that base modification selectively removes Si from the ash while the acid etching removes Al. This is reflected by the Si/Al ratio in the table. Treatment with more concentrated base and longer reaction times resulted in an even lower Si/Al ratio. The high chromium contents of samples MFA1 and MFA3 are the result of the high chromium content in the original ash (UFA1). The elemental composition for sample UFA2, however, is more representative of the fly ash produced in South Africa.[15]

3.2. Physical Characterization

The unmodified and modified samples exhibit similar mineralogy (Table 2). The zeolite phase Na-P1 ($Na_6Al_6Si_{10}O_{32}.12H_2O$)[16–20] was observed in samples MFA1 and MFA2 as secondary and

Table 2 Primary and secondary mineral phases identified in solids by XRD analysis.

Sample phase	UFA1	UFA2	MFA1	MFA2	MFA3
Mullite	Primary	Primary	Secondary	Primary	Primary
Feldspar	–[a]	–[a]	Primary	Primary	–[a]
Quartz	Primary	Primary	Secondary	Minor	Primary
Calcite	–[a]	–[a]	–[a]	Trace	–[a]
Dolomite	–[a]	–[a]	Minor	–[a]	–[a]
$Na_6Al_6Si_{10}O_{32}.12H_2O$	–[a]	–[a]	Secondary	Primary	–[a]

[a] Not observed.

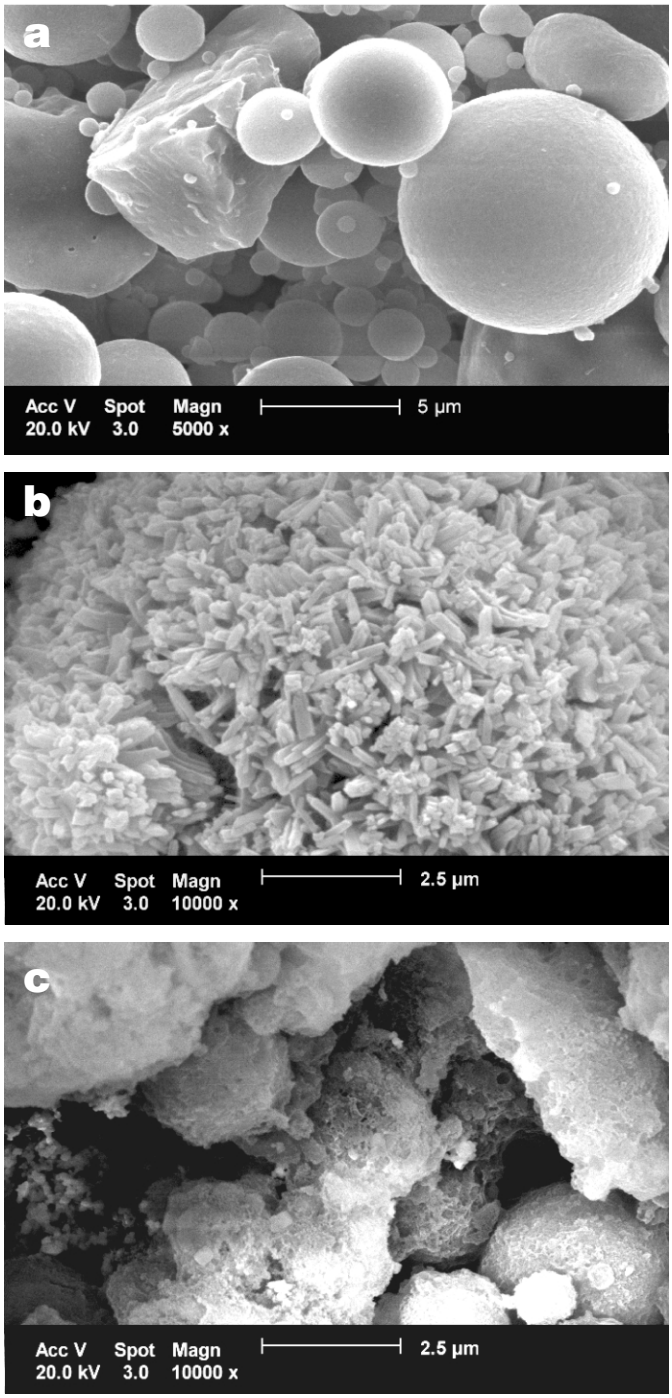

Figure 1 Scanning electron microscope pictographs of (**a**) unmodified fly ash (×5000), (**b**) base-modified fly ash (×10000) and (**c**) acid etched fly ash (×10000).

primary phases respectively. The presence of Na-P1 as a primary phase in MFA2 is consistent with the use of stronger base and longer reaction times. No trace of zeolite Na-P1 was observed in MFA3. This is because at low pH, aluminium ions are removed from the zeolite framework leading to the ultimate destruction of the structure.[21] Carbonate minerals (dolomite and calcite) were observed in the base-modified zeolite samples. Not surprisingly these minerals were leached by the acid treatment. This is corroborated by the elemental composition data (Table 1) in which the Ca and Mg concentrations decrease to near zero on acid treatment.

Scanning electron microscopy revealed that significant morphological changes were brought about by the modification procedures. Figure 1a indicates that the raw unmodified fly ash consists primarily of smooth spherical particles. These spheres are formed when the molten incombustible components in coal cool after combustion. EDS analysis revealed the angular particle in Fig. 1a to have the same composition as the spherical particles. It is likely that this particle may not have melted during combustion. Base treatment gave rise to polycrystalline spherulites, with irregular surfaces, exhibiting needle-like, outwardly radiating crystals (Fig. 1b). This is in agreement with observations for Na-P1 by a number of authors.[7,9,16,18,19] The crystallites formed during the modification process are small (most are $<1\,\mu$m). It has been noted that the presence of impurities has a significant influence on the crystal form produced during zeolite synthesis.[22] Because raw fly ash has large quantities of a host of elements, many of these will act as nucleation sites, which results in many small crystals rather than a few large ones. Acid etching removed the needle-like structures on the particle surfaces, revealing a porous underlying structure (Fig. 1c). This material is similar in appearance to amorphous silica.[10]

Table 3 Semi-quantitative atomic concentrations for the sample surfaces as determined by SXPS analysis.

Element	Concentration/atomic %				
	UFA1	UFA2	MFA1	MFA2	MFA3
C	12.1	12.0	5.9	9.3	4.0
O	60.0	58.6	56.5	57.7	69.4
F	–[a]	2.1	–[a]	–[a]	–[a]
Na	1.5	1.0	9.7	7.5	–[a]
Mg	2.5	0.2	3.5	2.7	–[a]
Al	9.5	8.5	5.3	6.3	–[a]
Si	12.7	14.7	18.1	12.8	26.6
S	–[a]	1.5	–[a]	–[a]	–[a]
Ca	1.6	1.4	1.0	3.0	–[a]
Si/Al	1.34	1.73	3.42	2.03	–[b]
Specific surface area/$m^2\,g^{-1}$	1.3	1.6	49	62	210

[a] Not observed.
[b] Not calculated.

SXPS results (Table 3) show that the surfaces of the base-modified ash samples exhibit a composition similar to that of the unmodified fly ash, the only difference being the relative abundance of the elements present. It can be observed that the surface of the unmodified ash contains a significant amount of graphitic soot from the combustion of coal. Part of this is removed during dissolution, since it is a very fine material which floats to the surface of the basic solution in which reflux takes place.

Surface Si/Al ratios, determined from SXPS results, suggest that the surface is enriched in Si compared with the bulk composition. This is because OH^- acts as a strong mineralizing agent for the quartz in the unmodified ash, which is then re-precipitated on the surface.[8,9]

The surface of sample MFA3 consisted mainly of SiO_2 and minor quantities of adventitious carbon or graphitic material. No aluminium was detected. The dealumination of surface aluminium from zeolites by mineral acids below pH 4 has been well reported.[23] The aluminium in the zeolitic materials, MFA1 and MFA2, is all exposed to the solution because of the channels present in the zeolite frameworks, and is thus susceptible to acid removal. Since the zeolites formed are at the surface of the fly ash, it is not surprising that SXPS (a surface technique) reveals no

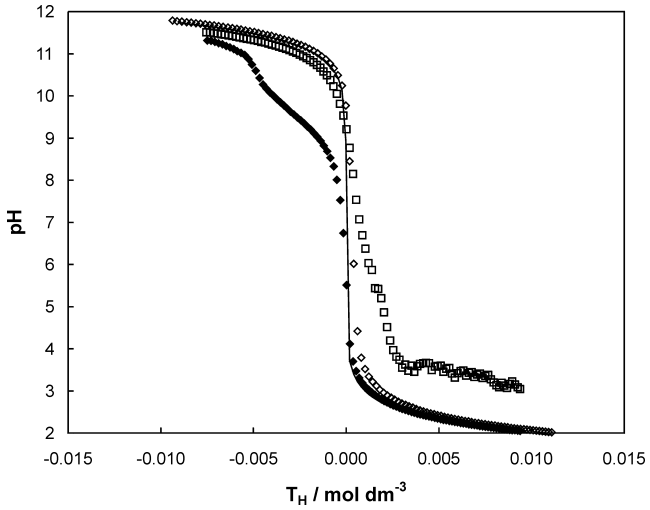

Figure 2 Typical examples of titration curves obtained for raw (♢), base- (□) and acid-modified (◆) fly ash samples. The solid curve is the blank titration.

Al at the surface. The residual Al that was found in MFA3 using XRF measurements (Table 1) represents Al that is still included in unreacted fly ash particles. It is thus not at the solid/solution interface and so is not as susceptible to acid attack.

A significant increase in specific surface area (Table 3) was observed for all modified samples. This is primarily due to the removal of cementitious material from pores. Similar observations were made by Lin and Hsi[7] and by Garde *et al.*[10] This effect is most pronounced for sample MFA3 where acid leaching removes material such as $CaCO_3$ that promotes agglomeration of particles.

3.3. Potentiometric Titrations

The displacement of suspension titration curves from a blank titration curve (Fig. 2) indicates that the modified solids are surface active. The untreated fly ash does not exhibit this behaviour to a significant extent, indicating a fairly unreactive surface.

3.4. Determination of Surface Protonation Constants

Surface parameters describing the acid-base chemistry of the surface-active samples are summarized in Table 4. The constants calculated for MFA1 and MFA2 are in close agreement. This is to be expected since similar XRD, SXPS and SEM data were obtained for these samples. Constants for MFA3 differ from those calculated for MFA1 and MFA2. The first is an acidic surface while the last two are alkaline surfaces. Comparison of the calculated constants with those of Hohl and Stumm,[24] Yoon *et al.*[25] and Sverjenski and Sahai[26] for ≡AlOH and ≡SiOH surface groups suggests that ≡AlOH groups are primarily responsible for the acid-base behaviour of MFA1 and MFA2 while, for MFA3, the acid-base characteristics are due to ≡SiOH surface groups.

SXPS data support the conclusions drawn above regarding the siliceous nature of the MFA3 surface. For MFA1 and MFA2, however, the surface Si/Al ratio calculated from SXPS data does not support potentiometric evidence that ≡AlOH surface groups are responsible for the surface acidity.

The pH at which the mineral surface changes sign is called the point of zero charge (PZC).[27] This can either be calculated from the estimated surface protonation constants or estimated from the experimental titration curves as the point at which the total hydrogen ion concentration, T_H (added acid concentration less added base), is zero. PZC values observed for MFA1 and MFA2 correspond with values observed for γ–Al_2O_3 (8.0 to 8.5) and gibbsite (9.0 to 9.8), compared with values of 1.8 to 3.8 observed for amorphous SiO_2 and quartz.[24–26] ≡AlOH and ≡SiOH surface groups have similar log K values for the reaction $XOH \rightarrow XO^- + H^+$, which suggests that the constant determined for the zeolitic material incorporates a contribution of both AlO^- and SiO^-. Arguing against this possibility is the observed PZC, which is higher than what might be expected if the surface consisted of both ≡SiOH and ≡AlOH groups. The experimental PZC (4.5) for the high surface-area quartz-mullite solid shows very good agreement with the value of 4.6 reported by Kita *et al.*[28] for a binary SiO_2-Al_2O_3 oxide. This would suggest that both ≡SiOH and ≡AlOH groups are responsible for surface protonation/deprotonation reactions for this solid.

Because the modelled and experimental PZC data do not fit properly (especially in the case of MFA3), it is impossible to reach firm conclusions regarding the exact nature of protonation sites on the zeolite-containing solids.

The site concentrations for MFA1 (0.9 mmol g^{-1}), MFA2 (1.0 mmol g^{-1}) and MFA3 (2.3 mmol g^{-1}) are in the range of cation exchange capacities (0.7–2.5 mmol g^{-1}) measured for similar zeolitized materials reported in the literature.[3,7,8,29] Interestingly, the site concentration for the Si-rich surface sample MFA3 lies within the range measured for amorphous SiO_2 by Yates *et al.*[30] (1.5–3.1 mmol g^{-1}).

3.5. Adsorption of Cu and Cd

Titration curves obtained in the presence of metal ions are shown in Figs 3 and 4. For MFA3, the titration curves show a distinct displacement from the protonation curves (Fig. 4), indicating that metal ion sorption liberates protons from the

Table 4 Summary of protonation constants and surface site concentrations for modified fly ashes.

	MFA1 (I = 0.3 mol dm^{-3})	MFA2	MFA3
log β (≡XO^-)[a]	–10.85 ± 0.0046	–10.76 ± 0.0045	–9.07 ± 0.0028
log β (≡XOH_2^+)[b]	7.78 ± 0.0051	8.08 ± 0.0043	1.27 ± 0.015
[≡XOH]/mol g^{-1}	(88.6 ± 1.9) × 10^{-5}	(102 ± 0.2) × 10^{-5}	(228 ± 0.4) × 10^{-5}
WSOS/DF[c]	297	118	131
n (number of data)	168	163	303
Sites/nm^2	10.9	9.9	6.5
ΔpK	3.1	2.68	7.8
PZC(Model)	9.1	9.1	5.4
PZC(Exp)	9.5	9.5	4.5

[a] Reaction is ≡$XOH \rightarrow$ ≡$XO^- + H^+$.
[b] Reaction is ≡$XOH + H^+ \rightarrow$ ≡XOH_2^+.
[c] Weighted sum of squares divided by number of degrees of freedom.

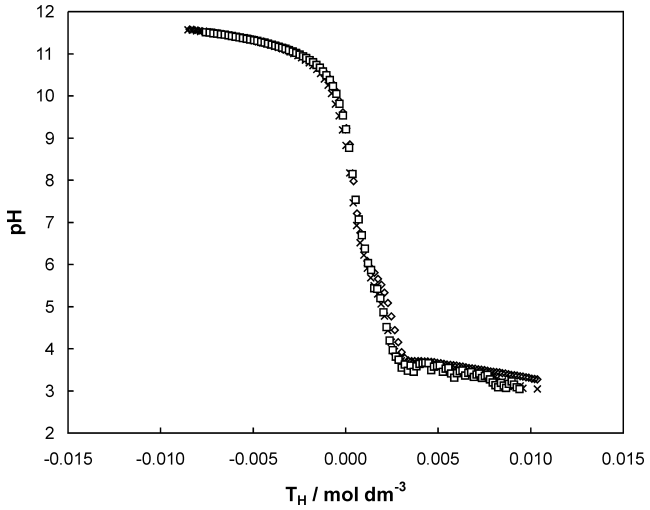

Figure 3 Typical titration curves obtained for the base modified solids in the presence of copper (x) and cadmium (◊). Also shown is a titration curve obtained with no metal present (□).

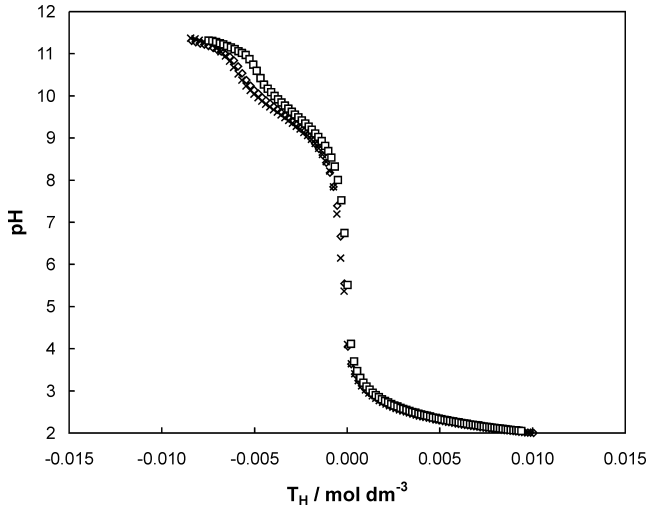

Figure 4 Typical titration curves obtained for the acid-modified solid (MFA3) in the presence of copper (x) and cadmium (◊). Also shown is a titration curve obtained with no metal present (□).

surface. For the zeolitic solids MFA1 and MFA2, no such displacement was observed (Fig. 3). This suggests that either metal sorption does not involve the liberation of H^+ ions from the surface or that no sorption occurs. This observation precluded the determination of surface complexation constants for Cu and Cd by the zeolitic solids.

Batch experiments of cadmium sorption by MFA2 as a function of pH and metal concentration showed that significant sorption did in fact occur (Fig. 5). A sorption capacity of 1.8 ± 0.3 mg g^{-1} was calculated at pH 5.7. At higher pH, almost 100% metal sorption was observed. Equilibrium simulations of the experimental systems using MINTEQA2,[12] however, suggested that the formation of a $CdCO_3$ precipitate may contribute to the observed sorption and thus sorption capacities were not calculated at these pH values.

Surface complexation constants for Cu and Cd by MFA3 are tabulated in Table 5. Copper and cadmium data could be satisfactorily modelled with the species ≡XOMOH. Surface speciation of 2.3×10^{-3} mol dm^{-3} metal was simulated using sorption constants and binding site concentrations obtained in this work. Calculations were performed using MINTEQA2.[12] A solids concentration of 1 g dm^{-3} was used, which is equivalent to a site concentration of 2.3×10^{-3} mol dm^{-3}. The speciation pattern for copper is shown in Fig. 6. Calculations suggest that copper is fully sorbed between pH 6 and 6.5. Above this pH range, the amount of copper sorbed decreases with increasing pH. The preferential formation of aqueous copper hydroxy species, as well as the formation of the solid, tenorite, leads to a decrease in the importance of the solid in removing copper from the solution phase. Simulation results yield a copper adsorption capacity of 146 ± 10 mg g^{-1} at pH 6. This is within the range reported for the cation exchange capacities of zeolitic materials synthesized from fly ash.[7,8,29,31]

The speciation pattern for cadmium is similar to that for copper. Cadmium sorption is complete at pH 7. Furthermore, the amount of cadmium adsorbed remained constant above pH 7, suggesting that aqueous cadmium hydroxy species are not successful in competing with the surface for available cadmium. A cadmium adsorption capacity of 258 ± 15 mg g^{-1} solid at pH 7 is suggested by the equilibrium calculations. This is again similar to the cation exchange capacities of zeolitic materials synthesized from fly ash.[7,8,29,31]

The high surface-area solid materials that have been synthe-

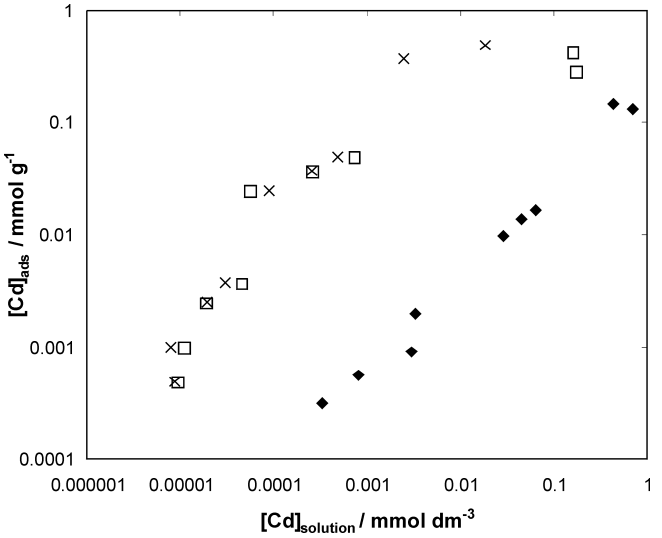

Figure 5 The sorption of Cd by base modified fly ash (MFA2) at pH = 5.7 (◆), 7.4 (□) and 9.5 (x) [Note: both axes are logarithmic].

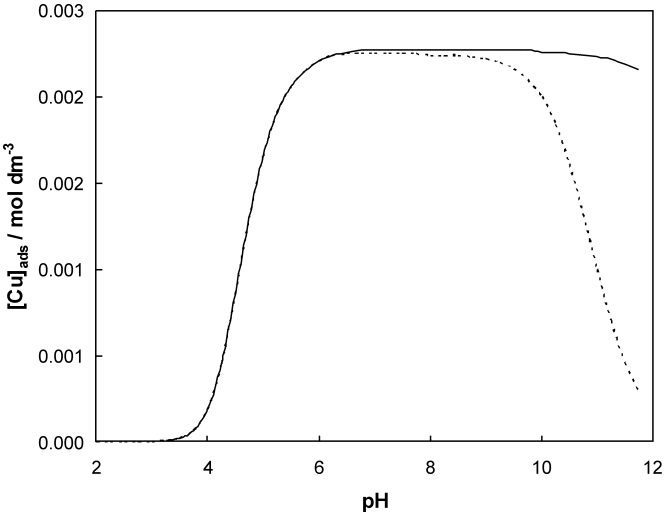

Figure 6 Speciation pattern showing the prevalence of the copper surface species (≡XOCuOH) as predicted from surface complexation parameters determined in this work for the adsorption of copper on MFA3 (concentration 1 g dm^{-3}). The dashed line illustrates the situation when tenorite is allowed to precipitate.

Table 5 Summary of metal adsorption constants determined for sorption by MFA3 and formation constants from MINTEQA2[12] used to model aqueous hydroxide species.

Copper speciation		Cadmium speciation	
Species	log β	Species	log β
OH^-	–13.85	OH^-	–13.85
H^+	0.00	H^+	0.00
Cu^{2+}	0.00	Cd^{2+}	0.00
$CuOH^+$	–7.36	$CdOH^+$	–9.94
$Cu(OH)_2$	–16.23	$Cd(OH)_2$	–20.38
$Cu(OH)_3^-$	–26.76	$Cd(OH)_3^-$	–33.16
$Cu(OH)_4^{2-}$	–39.02	$Cd(OH)_4^{2-}$	–46.78
$Cu_2(OH)_2^{2+}$	–9.78	$Cd_4(OH)_4^{4+}$	–30.56
		Cd_2OH^{3+}	–8.10
≡XO^-	–9.07[a]	≡XO^-	–9.07[a]
≡XOH_2^+	1.27[b]	≡XOH_2^+	1.27[b]
≡XOCuOH	–5.79[c]	≡XOCdOH	–6.14[c]

[a] Reaction is ≡XOH→ ≡XO^- + H^+.
[b] Reaction is ≡XOH + H^+→ ≡XOH_2^+.
[c] Reaction is ≡XOH + M^{2+} + H_2O → ≡XOMOH + $2H^+$.

sized by modification of fly ash with, firstly, concentrated base and then concentrated ash are capable of adsorbing metal ions at elevated pH (above 6). Adsorption is probably the result of complexation with hydroxyl groups on the silica-rich surface. By contrast, adsorption onto solely base-modified ash probably occurs via a cation exchange mechanism, since no deviation from the protonation curves was observed for the zeolitic solids MFA1 and MFA2. Here too, however, adsorption increased with increasing pH in batch experiments although it is possible that surface precipitation of metal carbonates and hydroxides takes place.

Both base- and base/acid-modified fly ash samples are potential sorbents for removing heavy metals from wastewater streams. The base-modified samples, however, will also result in high solution pH values, as observed by Amrhein *et al.*[3] This is because of the high PZC of this material. The material that was produced by the sequential base/acid treatment is thus more suitable because of its lower PZC and higher specific surface area. Unfortunately a caution needs to be added. The acidification step leads to a high leaching of heavy metals form the original ash and these need to be disposed of. It is possible, however, that this leachate may be used as a source for downstream electro-refining of some of these metals, in particular chromium and nickel.

4. Conclusions

High surface-area solids were synthesized from pulverized fly-ash samples originating from a South African power station. The surface characteristics of these solids suggest that ≡AlOH and ≡SiOH-type surface groups are responsible for their acid-base behaviour. Copper and cadmium are removed from solution by all the solids investigated. However, different mechanisms are suggested to be responsible for metal removal. Results suggest that the high surface-area quartz-mullite solid synthesized using a base and acid modification is more suitable than the zeolitic solid for use as a scavenger of heavy metal ions. It should be noted, however, that the synthesis of this solid unfortunately leads to a concentrated acid leachate which needs to be further processed.

Acknowledgements

The assistance of Unine Felix in performing the potentiometric titrations and synthesizing MFA2 is gratefully acknowledged. Kathy Garde is thanked for preparing samples MFA1 and MFA3. Alistair Douglas is thanked for assistance with the SEM photographs. Dr Richard Kruger, Ash Resources, supplied raw ash samples. P.J.P. acknowledges financial support from the Division of Water, Environment and Forestry Technology, CSIR, South Africa. C.D.W. acknowledges the assistance of the University of Port Elizabeth Research Committee and of the Foundation for Research Development, South Africa.

References

1 C.L. Carlson and D.C. Adriano, *J. Env. Qual.*, 1993, **22**, 227–247.
2 *Eskom Environmental Report*, Eskom, Johannesburg, South Africa, 2000.
3 C. Amrhein, G.H. Hagnia, T.S. Kim, P.A. Mosher, R.C. Gagajena, T. Amanios and L. de la Torre, *Environ. Sci. Technol.*, 1996, **30**, 735–742.
4 R.A. Kruger, *Fuel*, 1997, **76**, 777–779.
5 H. Höller and U. Wirsching, *Fortschr. Miner.*, 1985, **63**, 21–43.
6 M. Park and J. Choi, *Clay Science*, 1995, **9**, 219–229.
7 C-F. Lin and H-C. Hsi, *Environ. Sci. Technol.*, 1995, **29**, 1109–1117.
8 A. Singer and V. Berkgaut, *Environ. Sci. Technol.*, 1995, **29**, 1748–1753.
9 X. Querol, F. Plana, A. Alastuey and A. Lopez-Solar, *Fuel*, 1997, **76**, 793–799.
10 K. Garde, W.J. McGill and C.D. Woolard, *Plast. Rubber and Compos.*, 1999, **28**, 1–10.
11 H.F. McFarlane, K.M. Goff, F.S. Felicione, C.C. Dwight and D.B. Barber, *JOM*, 1997, **49**, 14–21.
12 J.D. Allison, D.S. Brown and K.J. Novo-Gradac, MINTEQA2/PRODEFA2, A Geochemical Assessment Model for Environmental Systems: Version 3.0 User's Manual, E.P.A./600/3-91/021, Environmental Research Laboratory, U.S. Environmental Protection Agency, Athens, USA, 1991.
13 D.A. Dzombak and F.M. Morel, *Surface Complexation Modelling: Hydrous Ferric Oxide*, John Wiley, New York, USA, 1990.
14 A. Herbelin and J.C. Westall, FITEQL: A Computer Program for Determination of Chemical Equilibrium Constants from Experimental Data, Version 3.1, Report 94–01, Oregon State University, Portland, OR, USA, 1994.
15 R.D. O'Brien, *The Neutralization of Acid Mine Drainage by Fly Ash*, M.Sc. thesis, University of Cape Town, Cape Town, South Africa, 2000.
16 C. Baerlocher and W.M. Meier, *Z. Kristallogr.*, 1972, **135**, 339–354.
17 R. Von Ballmoos and J.B. Higgins, *Zeolites*, 1990, **10**, 406S.
18 M.W. Grutzeck, *Ceram. Trans.*, 1996, **72**, 353–364.
19 M.W. Grutzeck and D.D. Siemer, *J. Am. Ceram. Soc.*, 1997, **80**, 2449–2453.
20 X. Querol, A. Alastuey, A. Lopez-Solar, J.M. Andres, R. Juan, P. Ferrer and C.R. Ruiz, *Environ. Sci. Technol.*, 1997, **31**, 2527–2533.
21 D.W. Breck, *J. Chem. Educ.*, 1964, **41**, 678–689.
22 J.C. Jansen, in *Introduction to Zeolite Science and Practice* (H. Van Bekkum, E.M. Flanigen and J.C. Jansen, eds.), Elsevier, Amsterdam, Netherlands, 1991, pp. 77–136.
23 R. Szostak, in *Introduction to Zeolite Science and Practice* (H. Van Bekkum, E.M. Flanigen and J.C. Jansen, eds.), Elsevier, Amsterdam, Netherlands, 1991, pp. 153–199.
24 H. Hohl and W. Stumm, *J. Coll. Interf. Sci.*, 1976, **55**, 281–288.
25 R.H. Yoon, T. Salman and G. Donnay, *J. Coll. Interface. Sci.*, 1979, **70**, 483–493.
26 D.A. Sverjenski and N. Sahai, *Geochim. Cosmochim. Acta.*, 1996, **60**, 3773–3797.
27 D. Langmuir, *Aqueous Environmental Geochemistry*, Prentice Hall, Upper Saddle River, NJ, USA, 1997, p. 351.
28 H. Kita, N. Henmi, K. Shimazu, H. Hattori and K. Tanabe, *J. Chem. Soc. Faraday Trans.*, 1981, **77**, 2451–2463.
29 C.D. Woolard, K. Petrus and M. van der Horst, *Water SA*, 2000, **26**, 531–536.
30 D.E. Yates, F. Grieser, R. Cooper and T.W. Healy, *Aust. J. Chem.*, 1977, **30**, 1655–1660.
31 H-L. Chang and W-H. Shih, *Ind. Eng. Chem. Res.*, 1998, **37**, 71–78.